J Mater Sci (2019) 54:2351–2357

Electronic materials

Silicon microstructures through the production of silicon nanowires by metal-assisted chemical etching, used as sacrificial material

O. Pérez-Díaz[1], E. Quiroga-González[1,*], and N. R. Silva-González[1]

[1] Institute of Physics, Benemérita Universidad Autónoma de Puebla, P.O. Box J-48, 72570 Puebla, Mexico

Received: 20 March 2018
Accepted: 8 October 2018
Published online: 15 October 2018

ABSTRACT

A simple, inexpensive and wafer-scale method to obtain Si microstructures is proposed. The method consists in a sequence of steps that include a selective metal-assisted chemical etching process to create regions of Si nanowires that are sacrificed in a post-etching process, leaving microstructures standing. As a proof of concept, Si micropillars with length of 7 μm and diameter of 1.4 μm were fabricated. The advantage of the proposed method is its simplicity, allowing the production of microstructures in a basic chemical laboratory.

Introduction

Micromachining is the term commonly used to enclose the production of mechanical structures (for different purposes) with a dimension ranging from 0.1 to 999 μm. It consists of combinations of material processing techniques, which can be grouped in three: (1) bulk micromachining, (2) LIGA (German abbreviation meaning lithography, galvanoforming and plastic molding) and (3) surface micromachining [1, 2]. From these, surface micromachining is the most commonly used for semiconductors. It consists in fabricating structures by one or multiple steps starting with the deposition of a masking layer, patterned by photolithography, and etching the unmasked sections. This etched material is named "sacrificial layer" [3–5]. Sacrificial layers are commonly used to produce freestanding structures like cantilevers and membranes. They just have to allow their selective removal [6, 7]. The deposition of these films is an important factor to consider when evaluating the final cost of the devices, since it is common that special facilities and complex equipment are required for this purpose, for example, when depositing by PECVD or sputtering.

Many materials have been proposed as sacrificial layers, such as Al [8], polysilicon [9], SiO_2 [10], Si_3N_4 [11], porous Si [12, 13] and Si nanowires [14]. In particular, sacrificial regions of Si (porous Si or Si nanowires) produced by etching are not widely used in microelectronics, but are a good candidate since no complex equipment is necessary for their production.

Si nanowires have been used as sacrificial material for the production of other structures like nanotubes [15] and metallic bridges [16]. They can be produced by a broad number of techniques, including the

Address correspondence to E-mail: equiroga@ieee.org

https://doi.org/10.1007/s10853-018-3003-z

metal-assisted chemical etching (MACE) technique, which is of special interest [17, 18]. Besides the production of Si nanowires, this technique has allowed the production of Si microstructures [19] and 3D nanostructures [20]. Its most important characteristics are its simplicity (it can be carried out in chemical laboratories without special equipment, such as potentiostats for electrochemical etching [21, 22]), and the fact that it can be performed at room conditions. To allow the MACE processing, noble metal (mainly Ag, Au and Pt) spots are previously deposited on the Si surface by different methods which includes thermal evaporation [23, 24], sputtering [25], electron beam evaporation [26], electroless deposition [27] and spin coating [28]. Among these techniques, the electroless deposition is the easiest technique since there is no need of any kind of equipment and the whole process can be carried out at room conditions. Additionally, this deposition method is scalable to the size of the substrate without complex optimization processes. However, it is important to mention that due to the nature of the deposition, a dispersion of sizes and shapes of the deposited particles could be expected.

The MACE process for Si etching can be described in the following way: a Si sample with metal is immersed in an HF-based solution. The metal sinks in the semiconductor leaving a pore behind, of the same shape and size than the metallized section. This happens because the metallized Si sections are etched much faster than the uncovered ones, due to the catalytic effect of the metal.

MACE has been used to produce microstructures even without masking or sacrificial layers. However, producing micron-sized isolated sections is tricky, since the patterned metallic layers used for etching must be completely homogeneous in thickness; any inhomogeneity could cause the metal sinks in a non-vertical way [29]. Furthermore, depositing flat and homogeneous metal films requires expensive equipment like sputtering. In the present work, a new method for fabricating Si microstructures is presented. It consists of producing sections (defined by photolithography) of Si nanowires by MACE, which act as sacrificial material that is dissolved in a KOH-based solution at the end of the process to leave microstructures behind (sections without nanowires). The advantage of this method is that it allows the fabrication of structures from microns to hundreds of microns, even when the size and shape of the noble metal particles used for the process are not homogeneous. The whole process can be carried out without the necessity of complex and expensive equipment.

Experimental section

For the preparation of the structures, pieces of 6-inch *p*-type (100) Si wafers with resistivity of 15–25 Ω cm were used. The method to obtain Si nanowires and the subsequent Si microstructures consists of the following steps:

(a) Patterning photoresist on Si wafer pieces by photolithography (Fig. 1a).
(b) Chemical deposition of metal (Ag in this work) particles (Fig. 1b).
(c) MACE etching process in an HF–H_2O_2-based solution to produce areas (defined by lithography) with Si nanowires (Fig. 1c).
(d) Etching away Si nanowires in a KOH-based solution (Fig. 1d).

A pattern is transferred to a photoresist, previously deposited on the Si sample. In our case, a quadratic array of circles of 1.5 μm of diameter is transferred on the wafer, with a pitch of 3 μm. Si surface sections covered with photoresist act as a masking layer allowing the metal deposition and the subsequent etching process only on the uncovered sections. Ag particles are deposited on the naked sections by immersing the sample in a solution composed of a volume proportion 50: 1 of $AgNO_3$ 0.1 M aqueous solution: HF 48%.

The deposition is for 3 min, to obtain particles big enough to coalesce leaving interstices for the production of Si nanowires and for the diffusion of the etchant. It is important to mention that other metals like Au and Pt can be deposited in a similar way and work also good for MACE [30]. However, in this work Ag was selected to minimize costs.

After the particles are deposited onto the Si surface, the sample is etched by MACE immersing it in an aqueous solution containing HF 48%, H_2O_2 30% as oxidant agent [31], and deionized water, in a proportion 4: 0.5: 35.5 v/v at 30 °C. Si nanowires are produced in the voids between Ag particles. Up to this point, sections of Si nanowires are obtained, and Ag particles remain at their bottom. The etching rate

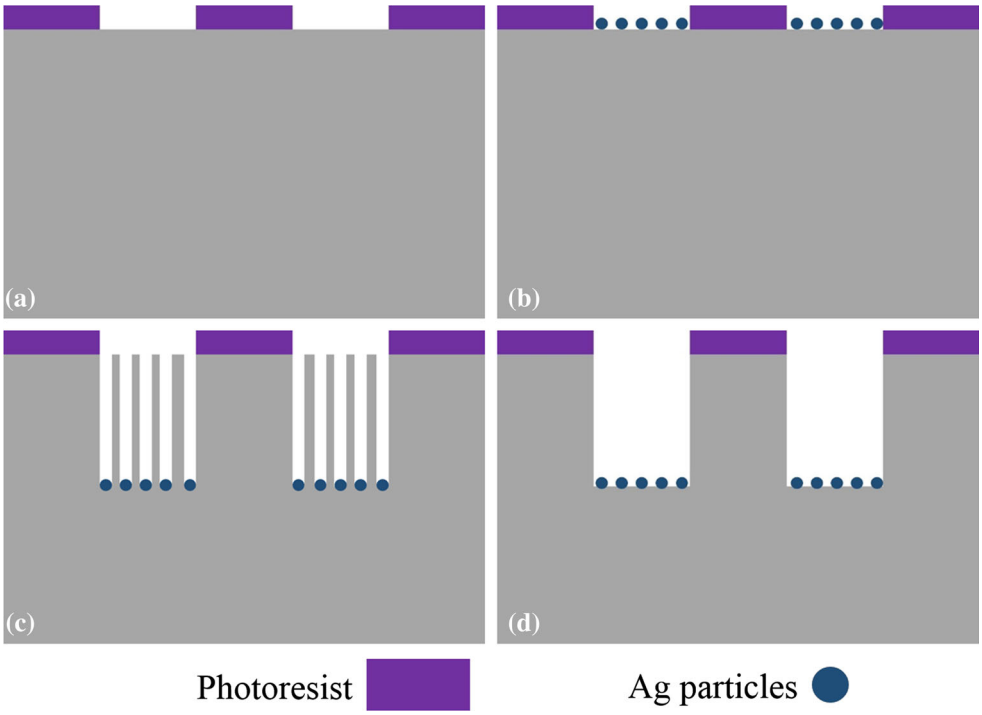

Figure 1 Steps to obtain Si structures by the here introduced method: **a** lithography process, **b** deposition of Ag particles, **c** metal-assisted chemical etching to produce Si nanowires, **d** chemical etching to dissolve the Si nanowires, resulting in Si microstructures.

is 30 μm/h. For obtaining the microstructures, it is necessary to remove these nanowires. For this purpose, the sample is immersed in a 0.25% wt aqueous solution of KOH at 50 °C [32, 33].

For this work, samples obtained at different stages of the fabrication process were analyzed with a field emission scanning electron microscope JEOL JSM-7500F.

Results and discussion

Figure 2 shows a sample after a pattern of photoresist has been obtained by photolithography on a Si sample and Ag particles have been deposited on the uncovered Si sections. The circles correspond to the photoresist, and the parts between them correspond to Ag particles on Si. Ag^+ ions are reduced and form metallic Ag particles onto the uncovered Si. The reactions are stated below [34–36]:

$$HF \rightarrow F^- + H^+ \quad (1)$$

$$Si + 6F^- \rightarrow SiF_6^{2-} + 4e^- \quad (2)$$

$$AgNO_3 \rightarrow Ag^+ + (NO_3)^- \quad (3)$$

$$Ag^+ + e^- \rightarrow Ag^0\,(s) \quad (4)$$

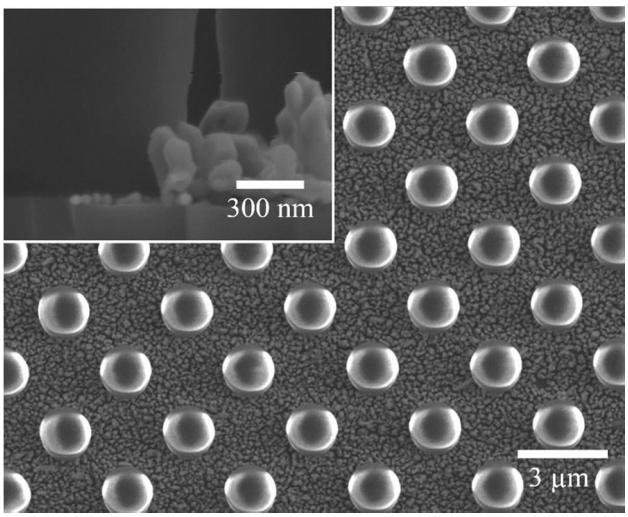

Figure 2 SEM micrograph of a Si sample with a quadratic pattern of circles of photoresist and Ag particles deposited on surface areas in between. Inset: cross section of the sample.

As can be seen in Fig. 2, the whole surface of the sample without photoresist is covered with Ag particles, which present a dispersion of sizes and shapes. The inset of the figure presents a cross-sectional SEM image of the sample, which evidences the dispersion of sizes. Figure 3 presents a histogram of the particle-size distribution. The most of the particles have sizes in the range from 51 to 150 nm; nevertheless, particles with sizes below this range are also present.

Various studies suggest that Ag particles with a diameter around 20 nm or less can etch into horizontal <110> directions or in a very erratic way [37–39]. However, this effect can be minimized when bigger particles are used [34].

In order to eliminate the smaller particles to minimize transversal or chaotic etching, a couple of processing steps are introduced after the deposition of Ag particles:

(a) The first one is to put the sample with Ag in an HF-based etching solution (with composition indicated in the section of experimental details) for 30 s in order to sink the particles into Si. The bigger particles sink more than the smaller ones. The reaction that takes place during this step is presented in (5) [36]:

$$Si + H_2O_2 + 6HF \rightarrow 2H_2O + H_2SiF_6 + H_2 \uparrow \quad (5)$$

H_2O_2 is reduced at the moment the Ag particles get in contact with the etchant; meanwhile, Si is oxidized at the metal–Si interface. SiO_x is continuously formed and then dissolved by HF, leading to the sinking of the Ag particles in Si. After the 30 s of etching, the particles are sunk about 300 nm (see Fig. 3).

(b) As a second step, the sample is immersed into an aqueous solution of HNO_3 and deionized water in a 1: 3 v/v ratio [40]. This step is to etch Ag. All the particles are affected by this reaction, but the smaller ones are etched faster, due to their larger surface-to-bulk ratio. As can be seen in Fig. 4, mostly big Ag particles are present after this step. To accomplish this result, it is important to implement step a). It is important to encrust the particles in Si, so that the biggest particles do not detach during the dissolution in HNO_3 and remain in their original position.

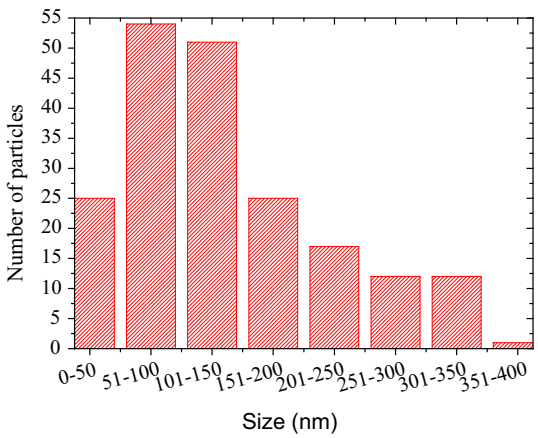

Figure 3 Ag particle-size distribution right after deposition.

An histogram of the particle-size distribution is presented in Fig. 5. As it can be seen in the figure, the particles below the 50 nm were almost completely removed. The most of the particles have sizes in the range from 51 to 200 nm, increasing the probability of vertical etching.

At this point, the sample is ready for the main etching, accomplished by immersing the sample in a new HF–H_2O_2 solution (composition indicated in the section of experimental details). Figure 6 presents a SEM micrograph of a sample after etching it for 10 min. The depth of the etched areas is 6 μm. The presence of Si nanowires and Ag particles (at the bottom) can be observed in the figure inset. It is clear that the etch front is not uniform, but it is expected due to the dispersion of shapes and orientations of the Ag particles, since the contact area of the Ag particles defines the etching profile [41]. It is important to mention that this effect may also occur when an Ag film is used instead of individual Ag particles [42].

The space between Ag particles results in nanowires, whose thickness is in the range from 90 to 300 nm. Additionally, Si micropillars can be seen. The pillars have some porosity at their top, due to

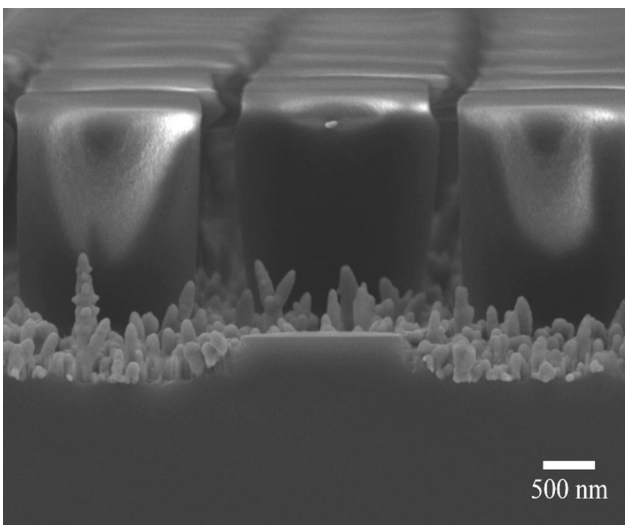

Figure 4 SEM micrograph of a sample after a fast etching step and the dissolution of the smallest Ag particles.

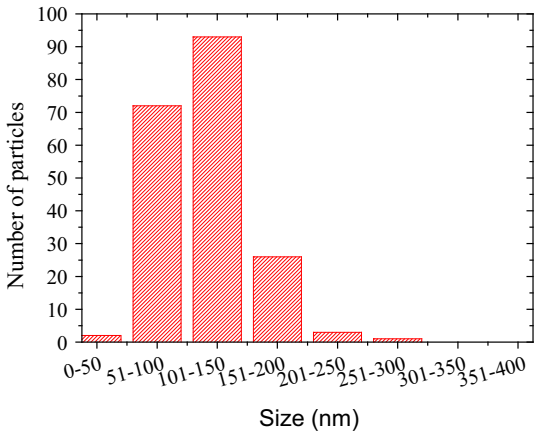

Figure 5 Particle-size distribution after the dissolution of the smallest particles.

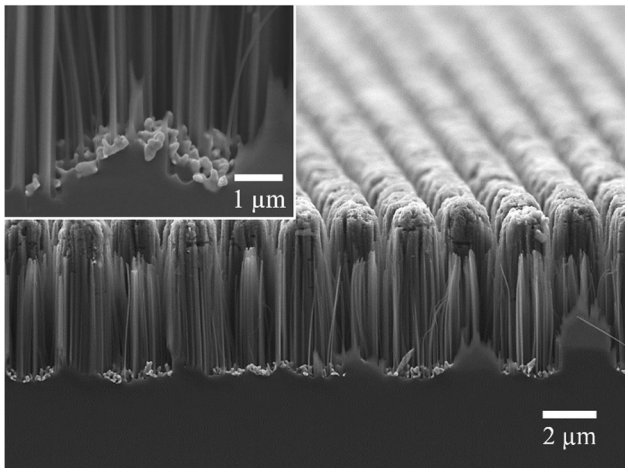

Figure 6 SEM micrograph of a sample after the etching process. Inset: zoom to the formed Si nanowires, with Ag particles at the bottom.

lateral etching caused by the remaining Ag particles with sizes below 50 nm. The photoresist is eliminated after the etching process.

To obtain the final microstructures, free of nanowires, these are sacrificed. As a final step, the sample is immersed into the KOH-based solution for 1.5 h. The whole sample is etched; nevertheless, as the Si nanowires are so thin, these are dissolved much faster than the Si microstructures (pillars in the present work).

The final structures are presented in Fig. 7. As it can be appreciated, the entire regions of Si nanowires were dissolved. The final length and diameter of the pillars are 7 and 1.4 μm, respectively. The top of the pillars was partially dissolved, since it was porous, and the pore walls were as thin as the Si nanowires. The walls of the Si micropillars present roughness given by the shape of the Ag particles. The interface between the sections with and the sections without particles is not even (its shape is related to the shape of the particles). After KOH etching, the walls look then faceted due to the anisotropic nature of the etchant. Using a longer etching may produce micropillars with smoother walls, but the top of the structures would also be dissolved. Some research groups have obtained similar structures by using metallic films or meshes for the etching process, without the need of an over-etching step (KOH etching in the present case); however, the structures are also partially dissolved at the top with even rougher walls [40, 43].

The present work is a proof of concept. The final etching process could also be performed in isotropic Si etchants. Additionally, depending on the application, the Ag particles laying at the bottom the structures could be dissolved in HNO_3 solutions.

The main advantage of the presented method relies in its simplicity. The use of complex equipment is not necessary for obtaining micropillars. The entire process can be applied at macroscale (for structures of hundreds of micrometers). For such applications, the defects associated with the metal particles would be unnoticed. The proof of concept of the present work reports structures obtained at the resolution limit; as the metal particles are in the range of 200 nm, and the structures are of about 1.4 μm, the curvature of the walls is evident and the shape of the Ag particles defines it.

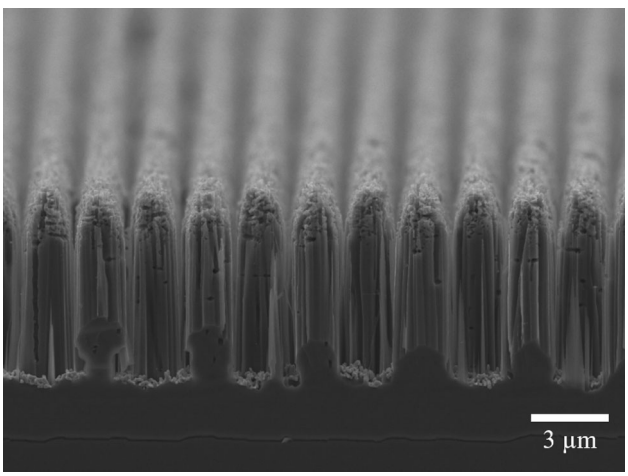

Figure 7 SEM micrograph of the obtained Si microstructures after the complete fabrication process.

Conclusion

An easy and inexpensive method to obtain Si structures was presented. Patterned regions of Si nanowires are produced by metal-assisted chemical etching (MACE) and are sacrificed in an over-etching process to leave Si microstructures remaining. The elimination of small Ag particles, used for MACE, allows vertical etching. The morphology of the walls of the microstructures strongly depends on the etchant used to dissolve the nanowires. Faceted structures are obtained in KOH solutions. The final structures reproduced the pattern of the photolithography mask. The whole process can be carried out at room temperature without complex equipment or special facilities, and it can be applicable at wafer scale.

Acknowledgements

This work was funded by Projects CONACyT INFR-2011-1-163153, CONACyT CB-2014-01-243407 and PROMEP BUAP-NPTC-377. The author O. Pérez-Díaz acknowledges the financial support of CONACyT through the scholarship with No. 378447.

Compliance with ethical standards

Conflict of interest All authors declare that they have no conflict of interest.

References

[1] Howe RT (1988) Surface micromachining for microsensors and microactuators. J Vac Sci Technol B 6:1809–1813

[2] Higurashi E, Ukita H, Tanaka H, Ohguchi O (1994) Optically induced rotation of anisotropic micro-objects fabricated by surface micromachining. Appl Phys Lett 64:62209–62210

[3] Sze S (2008) Lithography and etching. In: Sze S (ed) Semiconductor devices: physics and technology. Wiley, New York, pp 404–451

[4] Mahalik N (2008) Micromanufacturing and nanotechnology. Springer, Berlin

[5] Johnstone R, Parmaswaran A (2004) An introduction to surface-micromachining. Springer, New York

[6] Kusdterer J, Kohn E (2009) CVD diamond MEMS. In: Sussmann R (ed) CVD diamond for electronic devices and sensors. Wiley, London, pp 469–548

[7] Wolffenbuttel RF (1996) Development of compatible micromachining processes in silicon. In: Wolffenbuttel RF (ed) Silicon sensors and circuits: on-chip compatibility. Springer, London, pp 55–114

[8] Ataka M, Omodaka A, Fujita H (1993) A biomimetic micro motion system-a ciliary motion system. In: Proceeding of the international conference on transducers, Yocohama

[9] Shimaoka K, Tabata O, Kimura K, Sugiyama S (1993) Micro diaphragm pressure sensor using polysilicon sacrificial layer etch-stop technique. In: Proceeding of the international conference on transducers, Yokohama

[10] Jiang H, Yoo K, Yeh J, Li Z, Tien N (2001) Fabrication of thick silicon dioxide sacrificial and isolation blocks in a silicon substrate. J Micromech Microeng 12:87–95

[11] Lerner B, Perez M, Toro C, Lasorsa C, Rinaldi CA, Boselli A, Lamagna A (2012) Generation of cavities in silicon wafers by laser ablation using silicon nitride as sacrificial layer. Appl Surf Sci 258:2914–2919

[12] Yong D, Gwen L, Peng C, Litian L, Zhijian L (2002) Preparation and etching of porous silicon as a sacrificial layer used in RF-MEMSs devices. In: Proceedings of the international conference on solid-state and integrated-circuit technology, Shanghai

[13] Hedrich F, Billat S, Lang S (2000) Structuring of membrane sensors using sacrificial porous silicon. Sensors Actuators 84:315–323

[14] Amri C, Ouertani R, Hamdia A, Ezzaouia H (2018) Enhancement of electrical parameters in solar grade monocrystalline silicon by external gettering through sacrificial silicon nanowire layer. Mater Res Bull 98:41–46

[15] Convertino A, Cuscuna M, Martelli F (2012) Silicon nanotubes from sacrificial silicon nanowires: fabrication and manipulation via embedding in flexible polymers. Nanotechnology 23:305602

[16] Lee KN, Lee K, Jung S, Lee M, Seong W (2012) Fabrication of metal nanobridge arrays using sacrificial silicon nanowire. J Electr Eng Technol 7:396–400

[17] Li X, Bohn P (2000) Metal-assisted chemical etching in HF/H_2O_2 produces porous silicon. Appl Phys Lett 77:2572

[18] Liu K, Qu S, Zhang X, Wang Z (2013) Anisotropic characteristics and morphological control of silicon nanowires fabricated by metal-assisted chemical etching. J Mater Sci 48:1755–1762. https://doi.org/10.1007/s10853-012-6936-7

[19] Kim S, Khang D (2014) Bulk micromachining of Si by metal-assisted chemical etching. Small 10:3761–3766

[20] Hildreth O, Lin W, Wong C (2009) Effect of catalyst shape and etchant composition on etching direction in metal-assisted chemical etching of silicon to fabricate 3D nanostructures. ACS Nano 3:4033–4042

[21] Bell T, Gennissen P, DeMunter D, Kuhl M (1996) Porous silicon as a sacrificial material. J Micromech Microeng 6:361–369

[22] Weisse J, Lee C, Kim D, Cai L, Rao P, Zheng X (2013) Electro-assisted transfer of vertical silicon wire arrays using a sacrificial porous silicon layer. Nano Lett 13:4362–4368

[23] Fang H, Wu Y, Zhu J (2006) Silver catalysis in the fabrication of silicon nanowire arrays. Nanotechnology 17:3768–3774

[24] Huang Z, Fang H, Zhu J (2007) Fabrication of silicon nanowire arrays with controlled diameter, length, and density. Adv Mater 19:744–748

[25] Huang Z, Shimizu T, Senz S, Zhang Z, Zhang X, Lee W, Geyer N, Gösele U (2009) Ordered arrays of vertically aligned [110] silicon nanowires by suppressing the crystallographically preferred <100> etching directions. Nano Lett 9:2519–2525

[26] Chang S-W, Chuang V, Boles S, Ross C, Thompson C (2009) Densely packed arrays of ultra-high-aspect-ratio silicon nanowires fabricated using block-copolymer lithography and metal-assisted etching. Adv Funct Mater 19:2495–2500

[27] Peng K, Hu J, Yan Y, Wu Y, Fang H, Xu Y, Lee S, Zhu J (2006) Fabrication of single-crystalline silicon nanowires by scratching a silicon surface with catalytic metal particles. Adv Funct Mater 16:387–394

[28] Harada Y, Li X, Bohn P, Nuzzo R (2016) Catalytic amplification of the soft lithographic patterning of si nonelectrochemical orthogonal fabrication of photoluminescent porous si pixel arrays. J Am Chem Soc 123:8709–8717

[29] Hildreth O, Brown D, Wong C (2011) 3D Out-of-plane rotational etching with pinned catalysts in metal-assisted chemical etching of silicon. Adv Funct Mater 21:3119–3128

[30] Yae S, Morii Y, Fukumuro N, Matsuda H (2012) Catalytic activity of noble metals for metal-assisted chemical etching of silicon. Nanoscale Res Lett 7:352–356

[31] Chartier C, Bastide S, Lévy-Clément C (2008) Metal-assisted chemical etching of silicon in HF–H_2O_2. Electrochim Acta 53:5509–5516

[32] Yun M (2000) Investigation of KOH anisotropic etching for the fabrication of sharp tips in silicon-on-insulator (SOI) material. J Korean Phys Soc 37:605–610

[33] Quiroga-González E, Ossei-Wusu E, Carstensen J, Föll H (2011) How to make optimized arrays of si wires suitable as superior anode for li-ion batteries. J Electrochem Soc 158:E119–E123

[34] Peng K, Fang H, Hu J, Wu Y, Zhu J, Yan Y, Lee S (2006) Metal-particle-induced, highly localized site-specific etching of Si and formation of single-crystalline Si nanowires in aqueous fluoride solution. Chem Eur J 12:7942–7947

[35] Abouda-Lachiheb M, Nafie N, Bouaicha M (2012) The dual role of silver during silicon etching in HF solution. Nanoscale Res Lett 7:455–459

[36] Bastide S, Quang N, Monna R, Lévy-Clément C (2009) Chemical etching of Si by Ag nanocatalysts in HF–H_2O_2: application to multicrystalline Si solar cell texturisation. Phys Status Solidi C 6:1536–1540

[37] Li S, Ma W, Zhou Y, Chen X, Xiao Y, Ma M, Zhu W, Wie F (2014) Fabrication of porous silicon nanowires by MACE method in HF/H_2O_2/$AgNO_3$ system at room temperature. Nanoscale Res Lett 9:196–203

[38] Peng K, Lu A, Zhang R, Lee S (2008) Motility of metal nanoparticles in silicon and induced anisotropic silicon etching. Adv Funct Mater 18:3026–3035

[39] Tsujino K, Matsumura M (2007) Morphology of nanoholes formed in silicon by wet etching in solutions containing HF and H_2O_2 at different concentrations using silver nanoparticles as catalysts. Electrochim Acta 53:28–34

[40] Choi H, Baek S, Jang HS, Kim S, Oh B, Kim J (2011) Optimization of metal-assisted chemical etching process in fabrication of *p*-type silicon wire arrays. Curr Appl Phys 11:S25–S29

[41] Geyer N, Fuhrmann B, Leipner HS, Werner P (2013) Ag-mediated charge transport during metal-assisted chemical etching of silicon nanowires. ACS Appl Mater Interfaces 5:4302–4308

[42] Um H, Kim N, Lee K, Hwang I, Seo J, Yu Y, Duane P, Wober M, Seo K (2015) Versatile control of metal-assisted chemical etching for vertical silicon microwire arrays and their photovoltaic applications. Sci Rep 5:11277

[43] Choi K, Song Y, Ki B, Oh J (2017) Nonlinear etch rate of au-assisted chemical etching of silicon. ACS Omega 2:2100–2105